

1 **Precise dating of Middle to Late Villafranchian mammalian paleofaunae**
2 **from the Upper Allier River Valley (French Massif Central)**
3 **using U-Pb geochronology on volcanic zircons.**

4
5 Jean-Louis Paquette^{a*}, Etienne Médard^a, Jean-Louis Poidevin^b, Pascal Barbet^a

6 ^a Université Clermont Auvergne, CNRS, IRD, OPGC, Laboratoire Magmas et Volcans, 63000
7 Clermont-Ferrand, France

8 ^b Rue Moulin de Binet, 63270 Vic le Comte

9
10 *Corresponding Author: J-Louis.Paquette@uca.fr

11
12 **Keywords:** U-Pb geochronology; volcanic zircons; Villafranchian; mammals; paleofauna.

13
14 **Abstract**

15 The French Massif Central represents one of the rare occurrences in Europe where lower
16 Pleistocene fossil deposits are associated to a substantial volcanic activity. Thanks to the abundance of
17 volcanic zircons in the differentiated products of the Monts-Dore / Guéry stratovolcano, we were able
18 for the first time to use U/Pb geochronology on zircon to precisely date lower Pleistocene fossil
19 deposits. Zircon, a weathering-proof heavy mineral, was dispersed over the landscape through Plinian
20 eruptions, and quickly reworked in fossil-bearing sedimentary deposits. Five Villafranchian fossil sites
21 in the Upper Allier River valley (French Massif Central) have been precisely dated: Chilhac
22 (MNQ17b, 2.285 ± 0.046 Ma), Mont Coupet (2.274 ± 0.032 Ma), Senèze (reference locality for

MNQ18, 2.100 ± 0.029 Ma, confirming the previously determined 2.18-2.10 Ma $^{40}\text{Ar}/^{39}\text{Ar}$ ages), Blassac-La Girondie (MNQ19, 1.946 ± 0.029 Ma), and Vazeilles (1.843 ± 0.028 Ma). These new chronological data constrain the duration of the MNQ18 in central France to about 200 ka. The confirmation of an old age for the Blassac-La Girondie deposit indicates that the MNQ19 biozone started significantly earlier than previously thought.

1. Introduction

Recent evolution of megafauna in Europe including human arrival is directly linked to ecological and climate variations over the last few million years (e.g., Kahlke et al. 2011, Palombo 2014). The Villafranchian mammal age, defined from fossil deposits at Villafranca d'Asti, Italy (Pareto 1865, Rook and Martínez-Navarro 2010) is a biochronological unit based on large mammal species that covers the key period between 3.5 and 1.0 Ma during which the current European fauna was established, including human migration to Europe, likely through the Caucasus region (e.g., Carbonell et al. 2008, Lordkipanidze et al. 2013). Within the Villafranchian, faunal evolution is characterized by the definition of lower level biozones, each transition between biozones being related to first appearance (FAD) or last occurrence (LAD) of key species. The most commonly used biochronological schemes for large European mammals in Europe are the Neogene and Quaternary Mammal zones (MNQ, Mein 1976; Guérin 1982; Guérin et al. 1990), and the Faunal Units (FU) (Azzarolli 1977, Palombo and Sardella 2007).

Biozones are, however, a tool that can only provide relative chronology (biochronology). Absolute chronology constraints are required to tie the faunal evolution to climate variations and compare faunal evolution from different places. The precise timing and duration of Western European mammal biozones is thus still poorly understood, due to the limited number of precise absolute chronological constraints. In this paper, we use zircon crystals to precisely date a series of Early to Middle Villafranchian deposits (MNQ17 to MNQ19 mammal biozones) from the Upper Allier River valley in

48 central France. Zircon is a highly resistant, high-temperature mineral widely used to date magmatic
49 and metamorphic formations, including silicic volcanic deposits. Compared to other minerals used by
50 absolute geochronology techniques (feldspars, amphiboles, micas), zircon is preserved during
51 weathering of volcanic deposits and subsequent transport and is reworked within secondary
52 sedimentary deposits. Dating of volcanic zircons provide a minimum age for clastic sedimentary
53 deposits, however, if transport processes are fast (cf. Pastre, 1987), the age of the sedimentary deposit
54 will be within error of the age of the volcanic zircons. U/Pb dating of volcanic zircons is thus an
55 excellent tool for dating sedimentary fossil deposits, complementary to the more commonly used
56 $^{40}\text{Ar}/^{39}\text{Ar}$ technique (e.g., Nomade et al. 2014b, 2016).

57 All the investigated Middle to Late Villafranchian faunae belong to the Gelasian age (2.588 to
58 1.806 Ma), the earliest part of the Pleistocene. In the French Massif Central, only three volcanic
59 provinces were active during that time, the Devès volcanic field, the Escandorgue volcanic field, and
60 the Mont-Dore / Guéry stratovolcano. The investigated sites are located on the northeastern edge of the
61 Devès volcanic field, formed by a series of Plio-Pleistocene, mostly basanitic, eruptions that produced
62 lava flows, strombolian scoria cones, phreatomagmatic maars and Surtseyan tuff-rings (Mergoïl and
63 Boivin 1993). A significant number of eruptions were dated by K/Ar geochronology (see compilation
64 in Mergoïl and Boivin 1993), and most of the current chronological constraints on the fossil sites
65 comes from relative chronology between the fossiliferous sediments and the basanitic flows. The
66 existing ages are however imprecise, with uncertainties of at least a few hundred thousand years.
67 While the Devès volcanic field (as well as Escandorgue) exclusively emitted mafic lava, highly
68 explosive, zircon-producing, silicic eruptions also occurred in the Mont-Dore / Guéry stratovolcano,
69 70 km to the northwest.

70 The Mont-Dore massif is a composite edifice formed by two stratovolcanoes (Baubron and
71 Cantagrel, 1980; Nehlig et al., 2001), the Guéry and Sancy stratovolcanoes. The Guéry stratovolcano
72 represents the oldest volcanic center, which emitted a large range of explosive volcanic products
73 between 3.85 and 1.45 Ma (Cantagrel and Baubron, 1983; Pastre and Cantagrel, 2001; Nomade et al.,

2014a). The Sancy stratovolcano (1.1-0.25 Ma, Nomade et al. 2012) is younger than the deposits investigated here. Given the short distance, and the highly explosive activity of the Mont-Dore / Guéry stratovolcano, thin tephra layers likely blanketed the area during each Plinian eruption. Tephra-bearing layers have been found in association with one of the investigated deposits, the Senèze fossil site, and provided a precise age for the faunal association through $^{40}\text{Ar}/^{39}\text{Ar}$ geochronology on magmatic feldspars (Nomade et al. 2014b). Pastre (1987) performed a detailed study of the repartition of heavy minerals in sediments and slope deposits around the Allier river valley and concluded that heavy minerals deposited by airfalls were quickly reworked into the sedimentary network. For example, during the Fv alluvial cycle, heavy minerals in proximal pyroclastic deposits and in contemporary fluvial sediments are identical, with mineral associations changing every few 10,000 years (Pastre 1987). Due to this fast turnover, by dating volcanic zircons within sedimentary or slope deposits, it is possible to date the deposits themselves, with small age uncertainties.

All $^{40}\text{Ar}/^{39}\text{Ar}$ ages from the literature cited in this paper have been recalculated assuming an age of 1.1891 Ma for the ACs standard (Niespolo et al. 2017) and using the Renne et al. (2011) decay constant, following the procedures described by Mercer et al. (2016). K/Ar ages were also corrected according to the decay constants of Renne et al. (2011) although changes are within the uncertainties. All uncertainties have been recalculated at the 2σ level.

2. Villafranchian fossil deposits in the Upper Allier River valley

2.1. Chilhac

The Chilhac fossil sites are located NE of the village of Chilhac, in the Rabioulet valley, a small tributary of the Allier river. Fossils were first discovered in 1875 by de Morteuil (Boule 1892a, Bout 1960) in slope deposits, but the exact location of the discoveries (referred to as « Chilhac I ») is unknown. Two fossiliferous sites were later excavated, Chilhac II on the right bank of the stream, and Chilhac III on the left bank of the stream (Beden and Guth 1970a; Bœuf 1983). The at least 10 m thick

Chilhac II sediments are composed of non-bedded sandstones (containing angular basalt, quartz and gneiss pebbles) and slightly bedded clay- and mica-rich layers. Their exact depositional environment is still debated, and they have been interpreted as sediments from a slow-moving stream (Boivin et al., 2010), lacustrine sediments (Fouris et al. 1991), or lahar deposits (Pastre 1987). The Chilhac III deposits are partly disordered and are interpreted as the product of a landslide event affecting the Chilhac II sediments and overlaying pyroclastic and surface deposits (Boivin et al. 2010).

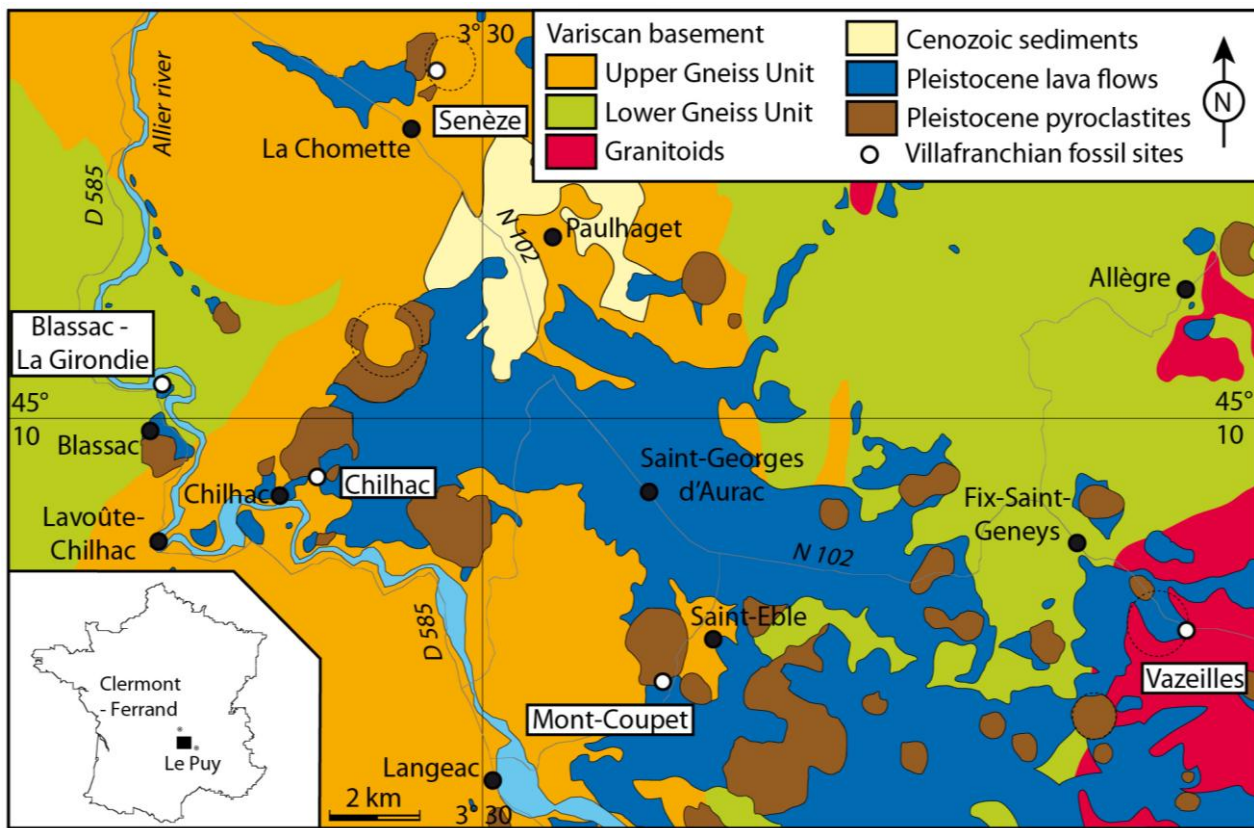


Figure 1. Simplified geological map of the investigated area, redrawn from BRGM 1/50 000 maps (Girod et al. 1979; Lasnier et al. 1981; Ledru et al. 1994; Marchand et al. 1986). The Paleozoic basement is partly covered by basanitic lava flows and pyroclasts belonging to the Devès volcanic field. Dashed circles are known maar structures, including the “Fressanges maar” (Vazeilles site, Séguy 1974) which was not known at the time the geological maps were drawn. Fossiliferous sites are contained within clastic sediments or slope deposits.

113

114 The two sites produced nearly identical fauna (Table 1, Beden and Guth 1970a, Boeuf 1983)
115 belonging to the MNQ17b biozone (Boeuf 1983, Palombo and Valli 2004). This fauna is more evolved
116 than the Saint-Vallier fauna (MNQ17a reference site, Saint-Vallier Faunal Unit, Guérin 1982, Guérin
117 et al. 2004, Palombo and Valli 2004), and is probably equivalent to the Coste San Giacomo Faunal
118 Unit of Italy (Palombo and Valli 2004, Bellucci et al. 2014). Possible archeological artefacts
119 (choppers) were found in the Chilhac III deposit (Guth 1974, Guth and Chavaillon 1985), but have
120 been later proven to be natural artefacts (Reynal et al. 1995).

121 The ages of the Chilhac deposits have never been precisely constrained. Based on the faunal
122 association (biostratigraphy), Boeuf (1997) favors an age close to 2.2 Ma. Both sites are arguably
123 younger than the 2.50 ± 0.12 Ma Pié des Varennes basanitic lava flow (K/Ar age from Couthures and
124 Pastre 1983), although the contact between the flow and the deposits is not visible (Boeuf 1997, Boivin
125 et al. 2010).

126 The Chilhac II site is surmounted by the Sognes basanitic lava flow (Boivin et al. 2010), in turn
127 covered by deposits from the Pié de Bouillergue scoria cone. K/Ar geochronology of the Sognes flow
128 by three different laboratories gives ages of 1.67 Ma (no error reported), 1.88 Ma (no error reported),
129 and 2.02 ± 0.60 Ma (compilation in Boeuf 1983). The age of 1.67 ± 0.10 Ma (Couthures and Pastre
130 1983) is further constrained by a reverse magnetic polarity (Prévôt 1975) that would place it after the
131 Olduvai subchron (i.e. younger than 1.780 Ma, Cohen and Gibbard 2019). More recently, a
132 centimetric, possibly reworked, trachytic tephra layer intercalated within scoria deposits from the Pié
133 de Bouillergue scoria cone, about 10 m above the top of the Chilhac fossil deposits, has been dated by
134 $^{40}\text{Ar}/^{39}\text{Ar}$ at 2.34 ± 0.08 Ma (Nomade et al. 2014b). According to this age, the fossil deposits would be
135 older than proposed by Boeuf (1997), between 2.50 and 2.34 Ma. We sampled sediments from the
136 fossiliferous levels of Chilhac II (sample CH2 coming from the Chilhac IIb dig, Table 2) and Chilhac
137 III (sample CH3), as well as the trachytic tephra layer previously dated by Nomade et al. (2014b)
138 (sample CHR).

			C	C	S	B	V
Proboscidea	Mastodontidae	<i>Anancus arvernensis</i>	x	x			
	Elephantidae	<i>Mammuthus meridionalis</i>	x	x	x	x	x
Perrisodactyla	Rhinocerotidae	<i>Stephanorhinus etruscus</i>	x	x	x	x	x
	Equidae	<i>Equus senezensis</i>			x	x	
		<i>Equus stenorhis guthi</i>	x	x	x		
		<i>Equus bressanus (Equus major)</i>		x	x	x	
		<i>Equus stehlini</i>			x		
	Tapiridae	<i>Tapirus arvernensis</i>		?			
Artiodactyla	Cervidae	<i>Libralces gallicus</i>			x		
		<i>Metacervoceros rhenanus philisi</i>	x	x	x		
		<i>Metacervoceros rhenanus perolensis</i>				x	
		<i>Croizetoceros ramosus</i>	x	x	x		
		<i>Eucladoceros ctenoides</i>	x	x	x		
		<i>Eucladoceros tetraceros</i>				x	x
		<i>Alces cf. carnutorum</i>				x	
	Bovidae	<i>Gallogoral meneghinii</i>	x		x		
		<i>Gazellospira torticornis</i>	x	x	x		
		<i>Hemitragus orientalis</i>			x		
		<i>Leptobos etruscus</i>		x	x	x	?
		<i>Leptobos furtivus</i>			x		?
		<i>Pliotragus ardeus</i>			x		
		<i>Megalovis latifrons</i>			x		
		<i>Procambtoceras brivatense</i>			x		
		<i>Eobison</i>			x		
	Suidae	<i>Sus strozii</i>		?	x		
Carnivora	Hyenidae	<i>Pliocrocuta perrieri</i>	x		x	x	
		<i>Chasmaporthetes lunensis</i>			x		
	Ursidae	<i>Ursus etruscus</i>			x	x	
		<i>Ursus minimus</i>	x				
	Canidae	<i>Canis arvensis</i>			x		
		<i>Canis etruscus</i>			x	x	
		<i>Nyctereutes megamastoides</i>	x		x		
		<i>Vulpes alopecoides</i>			x		
	Felidae	<i>Homotherium crenatidens</i>	x	x	x		
		<i>Acinonyx pardinensis</i>			x		
		<i>Megantereon cultridens</i>	x		x	x	
		<i>Felis sp.</i>				x	
Primates	Cercopithecidae	<i>Macaca sylvanus (florentinus)</i>			x		
		<i>Paradolichopithecus arvernensis</i>			x		

139

140

141

142

143

Table 1. Comparative list of large mammals described in the five investigated fossil deposits. The Chiljac list is reproduced from the compilation of Boivin et al. (2010), the Coupet list from Heintz (1974), the Senèze list from the work of Delson et al. (2006), the Blassac list from Beden and Guth (1970b) and Boeuf et al. (1992), and the Vazeilles list from Séguy (1974).

144

145 2.2. *Mont Coupet*

146 The Mont Coupet is a monogenetic volcano belonging to the Devès volcanic field. An initial
147 phreatomagmatic phase grades into a typical Strombolian scoria cone (Bout 1960). On the northern
148 side, a basanitic lava flow emerges at the base of the scoria cone. On the southern flank of the volcano,
149 weathered volcanic scoria forms a slope deposit up to 10-12 m thick (Dorlhac 1854, Bout 1960). This
150 slope deposit contains bones and bone fragments (Dorlhac 1854). A basanitic lava flow originating
151 from the neighboring Mont Briançon covers the lower part of the slope deposits (Bout 1970).

152 The Mont Coupet fossil deposit was discovered in 1849 (Aymard 1855). The fauna (Dorlhac
153 1854, Boule 1892a, Depéret et al. 1923, Heintz et al. 1974, Table 1) is very similar to the Chilhac
154 fauna and belongs to the MNQ17b biozone (Palombo and Valli 2004).

155 The lava flow associated with the scoria cone has been dated by K/Ar at 2.14 ± 0.18 Ma (Fouris et
156 al. 1991), providing an approximate upper limit for the age of the slope deposit. Bout (1970) reports a
157 1.9-1.8 Ma age for a lava flow from the neighboring Mont Briançon that covers the fossiliferous slope
158 deposits. We directly sampled the fossiliferous slope deposits (sample COU) to provide stronger
159 constraints on the age of this fossil site.

160

161 2.3. *Senèze*

162 The Senèze maar is a 500 m diameter phreatomagmatic crater belonging to the Devès volcanic
163 field. The crater was later filled by at least 123 m of lacustrine sediments comprising a lower layer of
164 sands (at least 43 m) and an upper layer of clays (Ehlai 1969, Roger et al. 2000). The upper
165 sedimentary layers are intercalated with and covered by slope deposits (Pastre et al. 2015).

166 The Senèze fossil deposits (Boule 1892b, Schaub 1943, Delson et al. 2006) are the reference
167 locality for the MNQ18 biozone (Guérin 1982, 1990, 2007). The rich mammalian paleofauna was

168 collected in the upper part of the lacustrine deposits and the associated slope deposits (Pastre et al.
169 2015).

170 The Lasnier basanitic flow, dated by K/Ar at 2.3 ± 0.3 Ma (Prévot 1975) or 2.55 ± 0.12 Ma
171 (Couthures and Pastre 1983), is closely associated with the maar but does not fill it, placing an upper
172 limit on the age of the phreatomagmatic eruption. A core drilled in the lacustrine sediments contained
173 a 5 cm thick tephra layer at a depth of 20.75 m that has been dated by $^{40}\text{Ar}/^{39}\text{Ar}$ at 2.11 ± 0.02 Ma
174 (Roger et al. 2000). Paleomagnetic data indicates that this tephra layer was deposited during the
175 normal Réunion subchron, and since the 19 m upper part of the core show reverse polarity, it is
176 younger than the end of the Réunion subchron at 2.116 Ma (Cohen and Gibbard 2019). This core is
177 unfortunately disconnected from the fossil-bearing layers, but the fossil deposits are assumed to be the
178 lateral equivalent of the upper part of the core, i.e. they would be younger than 2.11 Ma (Pastre et al.
179 2015). During the latest excavations of the slope deposits, Pastre et al. (2015) identified several layers
180 enriched in volcanic minerals and closely associated with the fossil deposits. In one trench, a layer
181 located a few decimeters below the main fossiliferous bed (sample SEN1) inside interstratified
182 lacustrine and slope deposits was dated by $^{40}\text{Ar}/^{39}\text{Ar}$ at 2.104 ± 0.050 Ma (Nomade et al. 2014b). A
183 short normal polarity anomaly, likely corresponding to the Réunion subchron, has been found just
184 above the dated layer (Sen in Nomade et al. 2014b), further supporting an age younger than 2.116 Ma
185 for the fossil deposit. In another of the recently excavated sites, fossiliferous lacustrine sediments were
186 framed by two layers, below (SEN98) and above (SEN101), dated at 2.176 ± 0.032 Ma and $2.132 \pm$
187 0.042 Ma, respectively (Nomade et al. 2014b). These ages are slightly older, but still consistent within
188 error with the fossiliferous level of the first trench. Two other slope deposits disconnected from the
189 fossiliferous layers were dated at 2.065 ± 0.020 Ma and 2.144 ± 0.044 Ma (Nomade et al., 2014b). We
190 sampled fossiliferous slope deposits on the edge of the crater (sample SEN), to put additional
191 constraints on the youngest possible age of the fossil deposits. The sample comes from a series of
192 alternating clays and sandy levels with centimetric pebbles, located less than 10 m from an outcrop of
193 granitic basement.

194

195 2.4. *Blassac-La Girondie*

196 The sedimentary sequence at Blassac-La Girondie crops out along the D585 road. It comprises
197 pebble-rich deposits interpreted as a lacustrine delta (Bout 1960), surmounted by approximately 1.5-
198 2.0 m of micaceous sands, in turn covered by 0.5-1.3 m of phreatomagmatic pyroclastic deposits, and a
199 40 m thick basanitic lava flow associated with the Pié Rouge scoria cone. Fossils were discovered at
200 Blassac-La Girondie in 1965 (Beden and Guth 1970b) at the base of the micaceous sand layer. These
201 fossiliferous sands are mostly of granitic origin (quartz-feldspar-biotite-muscovite), but are also
202 enriched in volcanic minerals, including green clinopyroxene, titanite, magnetite and zircon (Pastre
203 1987).

204 The Blassac fauna (Beden and Guth 1970b, Guth 1975) is younger than the MNQ18 fauna of
205 Senèze and has been correlated with the MNQ19 fauna of Peyrolles, based on the presence of Cervidae
206 remains similar to *Metacervoceros perolensis* (Beden and Guth 1970b, Heintz et al. 1974, Palombo
207 and Valli 2004). This interpretation was later challenged by the attribution of the remains to another
208 species, *Metacervoceros rhenanus* (Bœuf et al. 1992). *Metacervoceros perolensis* and *Metacervoceros*
209 *rhenanus* might actually belong to the same species (de Vos et al. 1995). A cluster analysis performed
210 by Palombo et al. (2006) indicates a very strong similarity between the Blassac-La Girondie and
211 Peyrolles fauna. Other evidence for Blassac-La Girondie belonging to MNQ19 includes the association
212 of *Stephanorhinus etruscus* and *Eucladoceros tetraceros*.

213 The basanitic flow overlying the fossil deposit has been dated by K/Ar at 2.06 ± 0.10 Ma
214 (Couthures and Pastre 1983) and 2.14 ± 0.12 Ma (Fouris et al. 1991), placing a lower limit on the age
215 of the Blassac-La Girondie fauna. A paleomagnetic study of the same flow gives a normal polarity
216 (Prévot 1975), suggesting it erupted during either the Olduvai subchron (1.925 to 1.728 Ma, Cohen
217 and Gibbard 2019), or the Réunion subchron (2.137 to 2.116 Ma, Cohen and Gibbard 2019). There is
218 an ongoing controversy between the geochronology data suggesting an old age, and the

219 paleontological data suggesting a correlation with the MNQ19 Peyrolles fauna that is assumed to be
220 much younger (1.449 ± 0.024 ; Nomade et al. 2014b). We sampled zircons from the fossiliferous level
221 (sample BLA) to get a more precise age for this deposit.

222

223 2.5. Vazeilles

224 The Vazeilles deposit (also called Vazeilles-Limandre or Fix-Saint-Geney) was discovered
225 during construction work on the N102 road between Brioude and Le Puy-en-Velay in 1974 (Séguy
226 1974). A sequence of lacustrine sediments (Figure 2) fills the crater of a maar volcano (“Fressanges
227 maar”) belonging to the Devès volcanic province (Séguy 1974; Fouris et al. 1991). The deposit is
228 comprised mostly of layers of clay, silt, sand, gravel, and diatomite with a steep bedding plane (17 to
229 45-degree dip towards the west). At the top of the deposit, a clay layer is covered by a basanitic lava
230 flow (Fouris et al. 1991).

231 Only a preliminary description of the paleofauna has been provided (Séguy, 1974): the sediments
232 contained fossils of *Stephanorhinus etruscus*, a molar of *Mammuthus meridionalis*, a few bovidae
233 bones (part of an astragalus and part of a tibia), and a molar from a large cervidae, possibly
234 *Eucladoceros*.

235 The basanitic lava flow situated on top of the deposit has been dated by K/Ar at 1.31 ± 0.12 Ma
236 (Fouris et al. 1991). The fossiliferous sediments have a normal magnetic polarity (Thouveny 1983),
237 whereas the polarity around 1.31 Ma was reverse (Matuyama chron). The youngest possible age for
238 the sediments thus corresponds to the Olduvai subchron (1.925 to 1.780 Ma). We sampled a layer of
239 gravel near the site where most fossils were discovered (sample VAZ1, Figure 2), and another sample at
240 the top of the sedimentary sequence (VAZ2), 1 m below the basanitic lava flow dated by Fouris et al.
241 (1991).

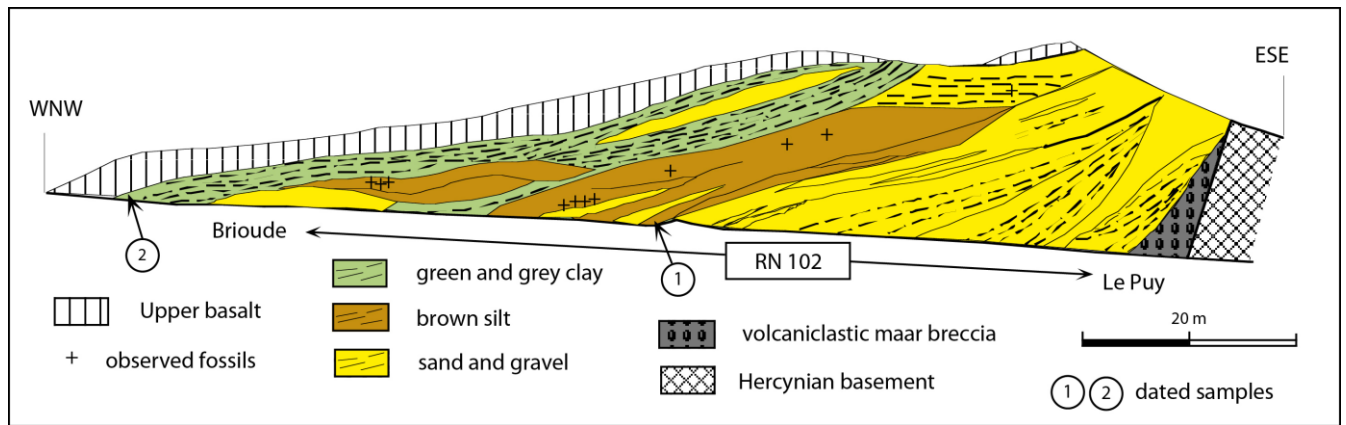


Figure 2. Cross-section of the Vazeilles deposits along the N102 road, redrawn from Séguy (1974).

3. U-Pb geochronology

3.1. Analytical technique

Between 1 and 10 kg of sediments were collected at each site. The sediment samples were cleaned and sieved, and zircons were separated from the 0.16-0.50 mm fraction by panning, magnetic separation and density separation using heavy liquids before handpicking under a binocular microscope. Zircons were then mounted in epoxy disks, ground, and polished with 0.25 μm diamond grit to expose crystal interiors. U-Th-Pb isotopic data on zircons were obtained by laser ablation inductively coupled plasma mass spectrometry (LA-ICP-MS) at LMV (Laboratoire Magmas & Volcans, Clermont-Ferrand, France). The analyses involved ablation of minerals with a Resonetics M-50 laser system operating at a wavelength of 193 nm. Spot diameters of 60 μm , repetition rates of 3 Hz and fluence of 3.0 J/cm^2 resulted in a spot depth of 12 μm (details in Supplementary Table S1). The ablated material was carried into helium and then mixed with nitrogen (Paquette et al., 2014) and argon before injection into the plasma source of a Thermo Element XR Sector Field high-resolution ICP-MS equipped with the jet interface pumping device. The alignment of the instrument and mass calibration were performed before every analytical session using the NIST SRM 612 reference glass, by inspecting the signals of ^{238}U , ^{232}Th and ^{208}Pb and by minimising the ThO^+/Th^+ ratio. The analytical method for isotope dating with laser ablation ICP-MS is basically similar to that reported in Hurai et

al. (2010) and Paquette et al. (2019). The ^{235}U signal is calculated from ^{238}U based on the ratio $^{238}\text{U}/^{235}\text{U} = 137.818$ (Hiess et al., 2012). Single analyses consisted of 30 seconds of background integration with laser off followed by 60 seconds integration with the laser firing and a 30 seconds delay to wash out the previous sample and prepare the next analysis.

Data were corrected for U-Pb fractionation occurring during laser sampling and for instrumental mass bias by standard bracketing with repeated measurements of GJ-1 zircon primary standard (Jackson et al., 2004). Repeated analyses of 91500 zircon reference material (Wiedenbeck et al., 1995) during each analytical session and treated as unknown, independently control the reproducibility and accuracy of the corrections. Data reduction was carried out with the software package GLITTER[®] from Macquarie Research Ltd (van Achterbergh et al., 2001; Jackson et al., 2004).

Schärer (1984) demonstrated that most zircons are affected during their growth by deficits and excesses of both ^{230}Th and ^{231}Pa relative to the initial Th/U secular equilibrium. In order to obtain accurate crystallization ages for young zircons (<10 Ma), it is necessary to correct for the effect of initial disequilibria caused by intermediate nuclides in the ^{238}U and ^{235}U decay series. Sakata et al. (2017) and Sakata (2018) propose a simplified correction model and a related Microsoft Excel spreadsheet based on the mathematical framework of Wendt and Carl (1985) using the following equations:

$$^{206}\text{Pb}^*/^{238}\text{U} = (e^{\lambda_{238} t} - 1) + \lambda_{238}/\lambda_{230} (f_{\text{Th/U}} - 1) (1 - e^{-\lambda_{230} t}) e^{\lambda_{238} t}$$

$$^{207}\text{Pb}^*/^{235}\text{U} = (e^{\lambda_{235} t} - 1) + \lambda_{235}/\lambda_{231} (f_{\text{Pa/U}} - 1) (1 - e^{-\lambda_{231} t}) e^{\lambda_{235} t}$$

The concentrations in U-Th-Pb are calibrated relative to the certified contents of GJ-1 zircon (Jackson et al., 2004) reference material. The available fractionation factor of Pa/U in a zircon-melt system of rhyolitic composition roughly shows agreement with a value of 2.9 ± 1.0 (Sakata, 2018, Paquette et al., 2019). Owing to the lack of any available magmatic protolith for the zircon sources, an estimated Th/U_{melt} value of 4.0 (Paquette et al., 2019) was systematically considered in the calculations as well as 50% uncertainties for the resulting individual $(\text{Th}/\text{U}_{\text{zircon}})/(\text{Th}/\text{U}_{\text{melt}})$ ratios. The isotopic

288 ratios and 2σ level uncertainties were corrected from elemental and isotopic fractionation, as well as
289 Pa/U and Th/U disequilibria. A systematic external error is subsequently propagated by quadratic
290 addition of uncertainties on U and Th decay constants as well as of the variability of the primary
291 reference material used for corrections (GJ-1) and of the long term variability of the secondary
292 reference material (91500). According to Horstwood et al. (2016), this systematic external error is
293 added to the 2σ error associated to the weighted mean $^{206}\text{Pb}/^{238}\text{U}$ ages calculation. The Tera and
294 Wasserburg (1972) diagrams were generated using Isoplot/Ex v. 2.49 software package by Ludwig
295 (2001).

297 *3.2. U-Pb zircon results*

298 The investigated samples are either sediments or slope deposits, and zircons are reworked either
299 from distal volcanic ash-falls, or from the local Variscan basement. Volcanic zircon crystals are light
300 pink, most often euhedral and may contain undetermined translucent inclusions. Variscan grains are
301 rather yellow with rounded shapes. The main analytical results are reported in Table 2.

303 3.2.1. Chilhac fossil deposits

304 For the Chilhac II sample, U and Th concentrations in the volcanic zircons are highly variable,
305 from 58 to 1050 ppm and from 39 to 5511 ppm, respectively. Th/U ratios are mostly higher than 1 up
306 to values about 5. Sixty spots were performed on the zircon grains including 39 spots in Pliocene
307 volcanic crystals and 21 spots in basement grains. A set of 34 Th/U disequilibria-corrected analyses
308 yields a weighted mean $^{206}\text{Pb}/^{238}\text{U}$ age of 2.285 ± 0.046 Ma (Fig. 3a), interpreted as the crystallization
309 age of the zircons. Crystals from the basement range from Carboniferous to Neo-Proterozoic (Fig. 5)
310 with one additional Neoproterozoic grain.

311 In the Chilhac III sample, U (59 to 886 ppm) and Th (55 to 3906 ppm) contents as well as Th/U
312 values (0.9 to 4.4) are broadly similar than in the previous Chilhac II sample. The fifty-four laser spots
313 were performed in 23 Pleistocene volcanic grains and 31 basement zircons. The volcanic zircons are
314 divided into two populations; the 17 younger ones yield a Th/U disequilibria-corrected mean
315 $^{206}\text{Pb}/^{238}\text{U}$ age of 2.262 ± 0.057 Ma (Fig. 4b), whereas six other zircons give an older mean $^{206}\text{Pb}/^{238}\text{U}$
316 age of 2.53 ± 0.10 Ma (Fig. 4b). Finally, the basement crystals provide the same age ranges than in
317 Chilhac II sample, from Carboniferous to Mesoarchean (Fig. 5a and b). The age of 2.26 Ma is
318 interpreted as the time of crystallization of the zircons in the magma chamber just preceding the
319 volcanic eruption. The age of 2.53 Ma could represent zircon grains related to an older unconstrained
320 event, or may also be the effect of data scatter resulting from U-decay induced damaged zircon crystal
321 parts. Even if this 2.53 Ma-old population mostly comprises low Th and U contents (<100 ppm),
322 additional dating of thermally and chemically annealed zircon crystals would be required to solve this
323 question (Von Quadt et al., 2014).

324 The upper trachytic airfall deposit contains only Neogene volcanic zircons for which the U ($404 \pm$
325 118 ppm) and Th contents (419 ± 220 ppm), as well as the Th/U ratios (1.0 ± 0.4) are more self-
326 consistent than in the two previous samples. Twenty-one of the twenty-three analysed laser spots yield
327 a Th/U disequilibria-corrected mean $^{206}\text{Pb}/^{238}\text{U}$ age of 1.727 ± 0.028 Ma (Fig. 4c). Interestingly, a
328 single zircon crystal at 2.56 Ma is synchronous within uncertainties with the older volcanic population
329 of the Chilhac III sample dated at 2.53 Ma.

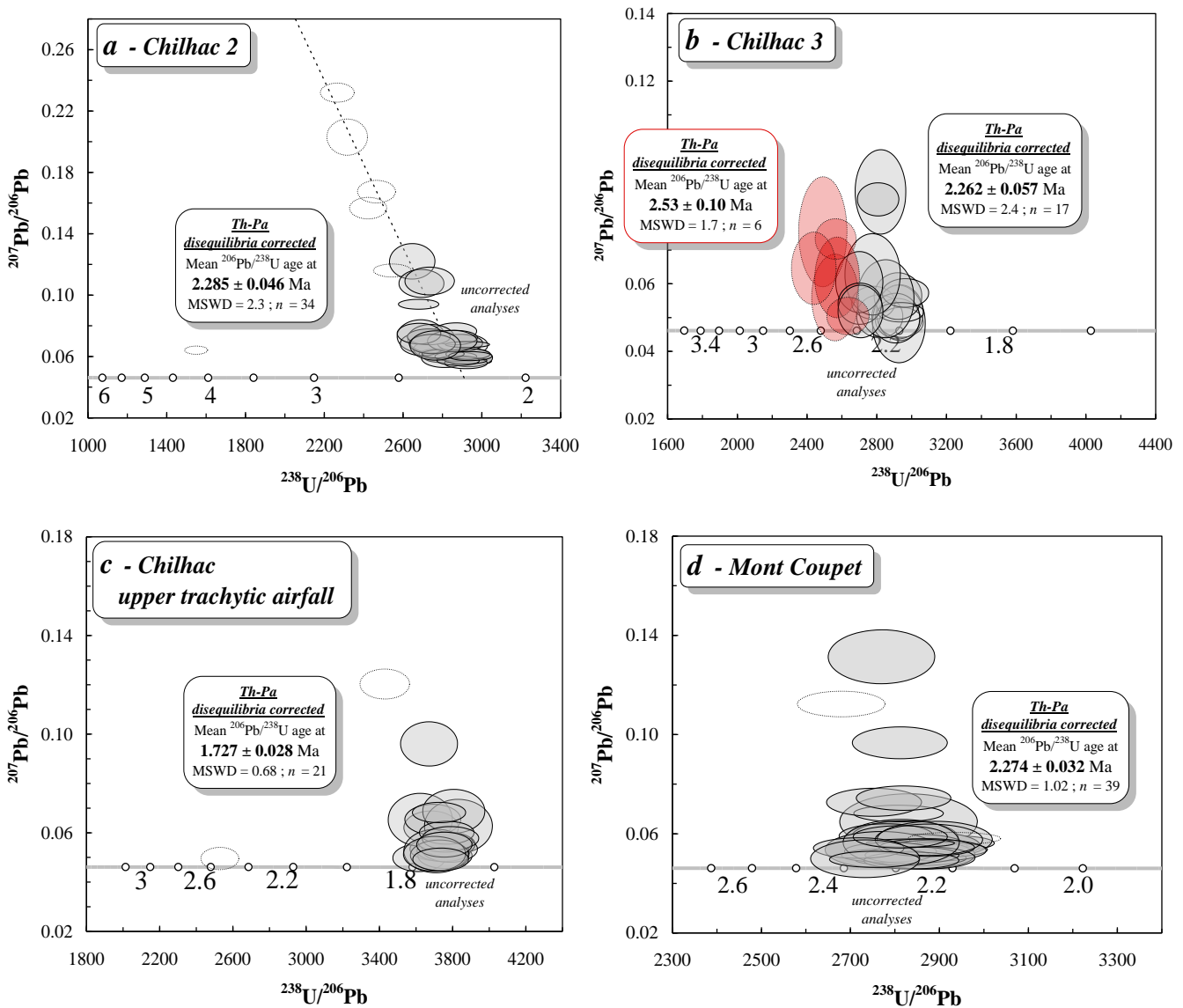
330 331 3.2.2. Mont Coupet slope deposits

332 In the Mont Coupet sample, the variable U (43 to 991 ppm) and Th (33-2483 ppm) contents are
333 comparable to that of the Chilhac II and III samples. Similarly, Th/U ratios (0.7 to 3.1) also display
334 significantly high values. Thirty-nine of the forty-one spot analyses yield a Th/U disequilibria-
335 corrected mean $^{206}\text{Pb}/^{238}\text{U}$ age of 2.274 ± 0.032 Ma (Fig. 3d), which is also, within uncertainties,

336
337

consistent with the ages measured on Chilhac II and III zircons. No other zircon crystals were recovered in that sample.

338



339

Figure 3. U/Pb diagrams for the investigated zircons from Chilhac and Mont Coupet fossil deposits. (a) and (b) are bulk sediments from the Chilhac deposits, (c) is the upper trachytic airfall located 10 m above the Chilhac III deposit, and (d) are slope deposits from Mont Coupet.

343

3.2.3. Senèze upper slope deposits

345

In the Senèze sample, U (85-1103 ppm) and Th (71-2651 ppm) are still variable as well as Th/U ratios (0.7 to 2.7). Fifty-two spots were performed on Pleistocene volcanic zircons and yield a Th/U

346

347 disequilibria-corrected mean $^{206}\text{Pb}/^{238}\text{U}$ age of 2.100 ± 0.029 Ma (Fig. 4a). Again, no basement zircons
348 were recovered in that sample.

349 350 3.2.4. Blassac-La Girondie sand

351 In the Blassac-La Girondie zircon crystals, U (59-450 ppm) and Th (45-542 ppm) contents are
352 lower than in the other samples and associated with rather constant Th/U (1.1 ± 0.4) values. Twenty-
353 five of the twenty-nine spots performed on the Pleistocene volcanic zircons yield a Th/U disequilibria-
354 corrected mean $^{206}\text{Pb}/^{238}\text{U}$ age of 1.946 ± 0.029 Ma (Fig. 4b). Eight basement zircons consistent with
355 the age range defined by the Chilhac samples (Fig. 5a and b) have been analysed.

356 357 3.2.5. Vazeilles sediments

358 In the zircon crystals from the Vazeilles fossiliferous sediments, the U (93-796 ppm) and Th (103-
359 1808 ppm) contents are high and comparable to those of Chilhac and Le Coupet samples with varied
360 igneous Th/U values (0.6-2.6). On the thirty-nine analyzed Pleistocene zircons, thirty-four grains yield
361 a Th/U disequilibria-corrected mean $^{206}\text{Pb}/^{238}\text{U}$ age of 1.843 ± 0.028 Ma (Fig. 4c). The five older
362 zircon crystals range between 320 Ma and 670 Ma.

363 In the Upper Level sample, the U (37-1077 ppm) and Th (51-2854) as well as Th/U ratios (0.7-
364 2.6) display varied and high values, similarly to the former sample. A large group of 42 on 46 analyses
365 yields a Th/U disequilibria-corrected mean $^{206}\text{Pb}/^{238}\text{U}$ age of 1.648 ± 0.025 Ma (Fig. 4d). The three
366 remaining zircon grains recorded ages of 580, 610 and 640 Ma, respectively (Fig. 5a).

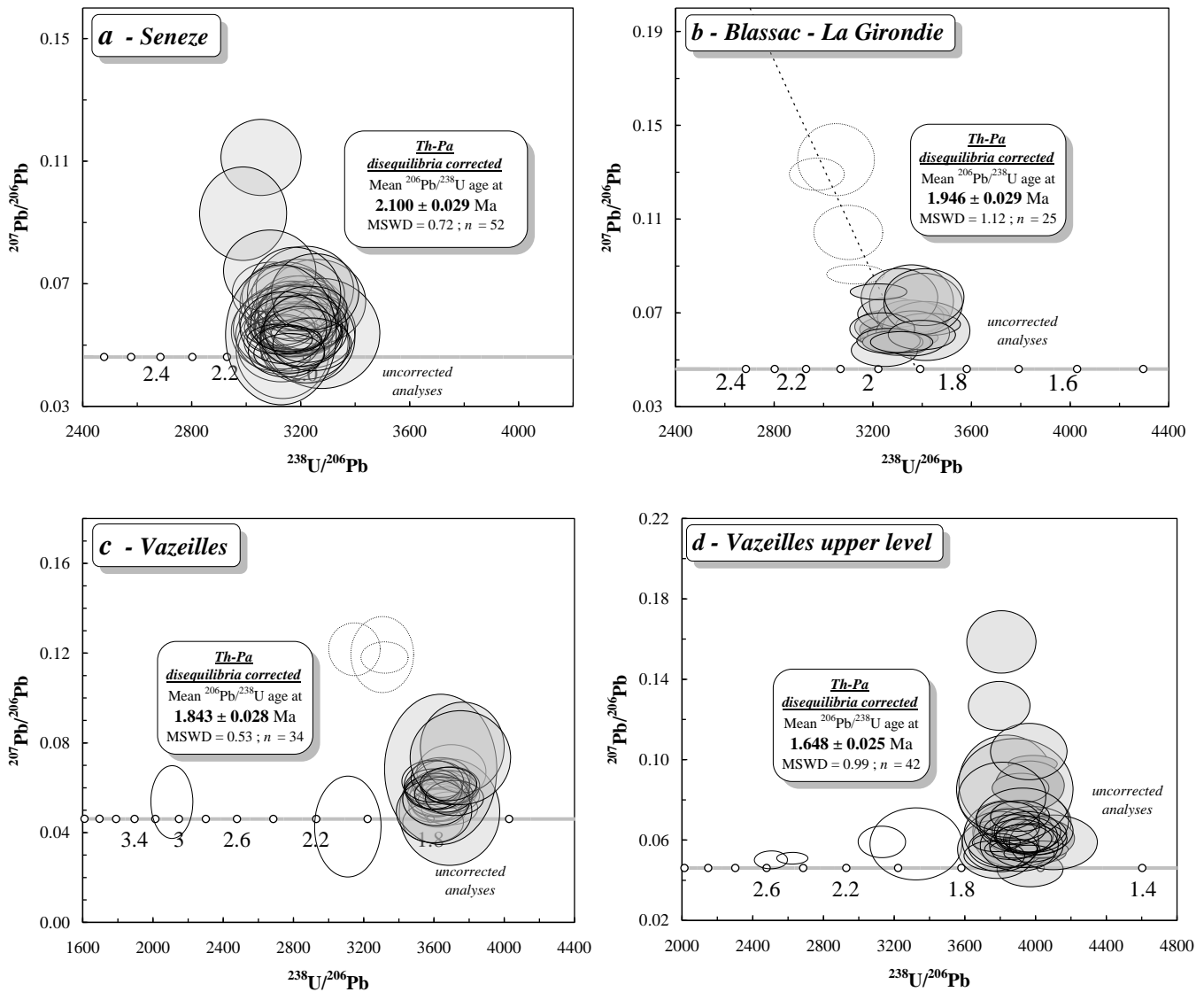


Figure 4. U/Pb diagrams for the investigated zircons from Senèze, Blassac-La Girondie and Vazeilles fossils deposits.

3.2.6. Older zircons from the Variscan basement

Sixty-eight zircons from the Chilhac II and III, as well as Blassac-La Girondie and Vazeilles samples are derived from the crystalline basement of the French Massif Central (Figure 5) and were either associated with the Neogene volcanic zircons during the volcanic eruptions or have been incorporated as detrital grains by late sedimentary processes. About half of this population (Figure 5b) defines a sharp Cambro-Ordovician (~480 Ma) peak, whereas a subordinate Carboniferous peak most probably records the crystallization of Hercynian granites. The Cambro-Ordovician ages are typical of

380 the protoliths of the Variscan Upper Gneiss Unit (e.g. Chelle-Michou et al., 2017), which constitutes
 381 the basement of the Chilhac area, and crops out upstream of the Blassac deposits, strongly suggesting
 382 that these zircons are detrital. An Ediacaran peak associated to the occurrence of Cryogenian and
 383 Archean grains is typical of the detrital zircon record related to the geodynamic evolution of the north
 384 Gondwana margin (e.g. Couzinié et al., 2019).

385

sample	X	Y	Z	Age (Ma)	2 σ error (Ma)
CH 2(II)	45°09'33.3''N	3°26'37.2''E	550 m	2.285	0.046
CH 3(III)	45°09'36.6''N	3°26'41.6''E	585 m	2.262	0.057
CHR	45°09'43.3''N	3°26'45.5''E	580 m	1.727	0.028
COU	45°07'12.7''N	3°32'39'8''E	615m	2.274	0.032
SEN	45°14'23.6''N	3°28'57.9''E	630 m	2.100	0.029
BLA	45°10'41.2''N	3°24'08.1''E	490 m	1.946	0.029
VAZ1	45°07'38.8''N	3°41'34.9''E	987 m	1.843	0.028
VAZ2	45°07'56.8''N	3°41'26.3''E	1010m	1.648	0.025

386

387 *Table 2. Sample location and U/Pb chronological data for the investigated fossil sites.*

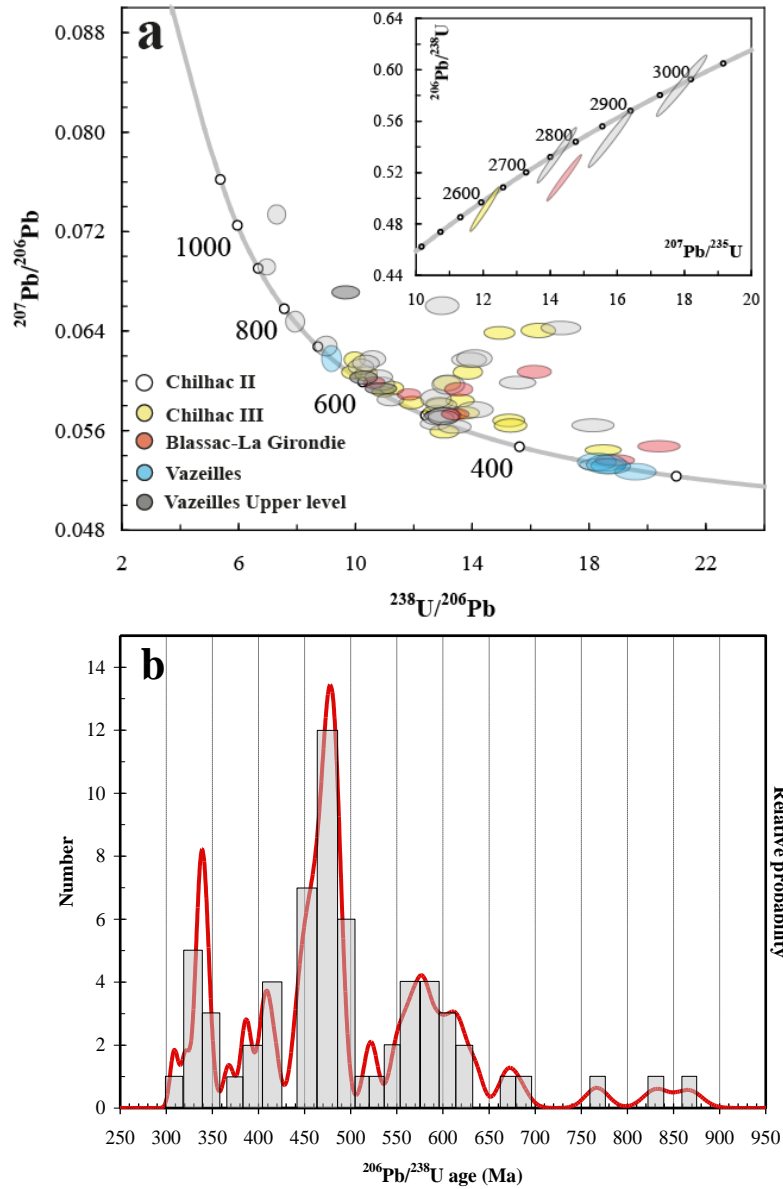
388

389 **4. Discussion**

390 *4.1. Constraining the age of sedimentary and slope deposits with volcanic zircons*

391 Since the investigated zircons are reworked from distal volcanic ash-falls, we should expect one or
 392 more zircon populations, with the youngest population providing a lower age for the sedimentary
 393 deposit. Proximal slope deposits (our samples from Mont Coupet and Senèze), indeed contain one
 394 single population of volcanic zircons with a well-constrained magmatic age (Figure 3d and 4a).

395



396
397
398 *Figure 5. Older ages measured in pre-Cenozoic zircons from the fossiliferous sediments a) The Tera-*
399 *Wasserburg plot represents the Proterozoic and Phanerozoic ages; the Concordia diagram in inset*
400 *shows the Archean ages; b) Cumulative probability ages histogram plot.*

401
402 Sediments sampling a large, active, river basin (Allier river sediments at Blassac-La Girondie) still
403 contain a dominant zircon population with a single magmatic age, and a small proportion of older
404 zircons (volcanic and from the basement). A more complicated history emerges from the Chilhac
405 deposits, which were formed in a small drainage system that eroded a variety of metamorphic and
406 volcanic deposits. The zircon population is, however, still characterized by a predominance of the

407 younger population age. These results confirm the conclusions of Pastre (1987) that heavy minerals
408 deposited by airfalls are quickly reworked into the sedimentary network. Given this fast renewal, and a
409 likely near-continuous volcanic activity from the Mont-Dore / Guéry stratovolcano, the highly
410 dominant youngest zircon population in each sample provides an age very close to the deposition age
411 of the sediment.

413 *4.2. New age constraints on major fossil deposits in volcanic context*

414 4.2.1. Chilhac fossil deposits

415 Zircons from both fossiliferous layers have statistically identical ages of 2.285 ± 0.046 Ma for
416 Chilhac II and 2.262 ± 0.057 Ma for Chilhac III, in agreement with the 2.2 Ma age proposed by Bœuf
417 (1997) based on the biochronological attribution to the MNQ17b biozone. Although no proximal
418 pyroclastic layer has been precisely dated in the Mont-Dore / Guéry stratovolcano between 2.5 Ma
419 (debris avalanches and lahars of the Perrier Plateau) and 2.07 Ma (Guéry tephra, Nomade et al. 2014a),
420 relative chronology of trachytic pyroclastic deposits in the Vendeix stream and the Bouay waterfall
421 sections indicate ages close to 2.3 Ma (Pastre and Cantagrel, 2001). These 2.27 Ma old zircons are thus
422 interpreted as products of a Plinian eruption whose deposits are present but have not yet been precisely
423 dated in the central part of the stratovolcano.

424 For the Chilhac samples, the number of old zircons is high (21/60 for Chilhac II, 31/54 for Chilhac
425 III), pointing to a significant sedimentary component from the metamorphic basement, in agreement
426 with the abundance of quartz and micas in the sediments. The Chilhac III sample also contains a
427 significant amount of reworked volcanic zircons crystals (2.53 Ma).

428 Nomade et al. (2014b) dated a trachytic tephra located stratigraphically above the Chilhac III
429 deposits by Ar/Ar and obtained an age of 2.34 ± 0.08 Ma, which would thus be a minimum age for the
430 deposit. However, zircon U/Pb ages for this deposit are significantly younger (1.727 ± 0.028 Ma),
431 suggesting that the feldspars dated by Ar/Ar might be xenocrysts older than the trachytic layer. This is

not uncommon and has been already described in the Monts-Dore for the « Grande Nappe » pyroclastic unit (Nomade et al. 2017). Also, the presence of metamorphic garnet, a mineral not seen in the proximal Mont-Dore deposits but widespread in the basement rocks of the Chilhac area might suggest that this unit is not a pristine ash-fall deposit and has been reworked. Our new results date this pyroclastic unit, and thus also the age of the Pié de Bouillergue scoria cone in which the layer is intercalated at 1.727 ± 0.028 Ma. This age is consistent with the K/Ar (1.67 ± 0.10 Ma, Couthures et Pastre 1983) and paleomagnetic (< 1.78 Ma, Prévôt 1975) age of the Sogne basanitic flow, and precisely constrains the age of the Pié de Bouillergue volcanic eruption. Once again, there are no known proximal pyroclastic deposits of that age in the Mont-Dore / Guéry stratovolcano, but no proof of an activity gap at that time either.

The new ages of 2.285 ± 0.046 Ma and 2.262 ± 0.057 Ma, identical within error (average 2.27 Ma), are much more consistent with previous paleontological estimates (e.g., Bœuf et al. 1992) than the > 2.34 Ma age proposed by Nomade et al. (2014b). They are in excellent agreement with the age of the similar Coste San Giacomo fauna of Italy (estimated at 1.95-2.2 Ma by Bellucci et al. 2014), confirming the equivalence of the MNQ17b biozone and the Coste San Giacomo Faunal Unit.

4.2.2. Mont Coupet slope deposits

The fossil deposits at Mont Coupet contain zircons with the exact same age as the Chilhac fossil sites, 2.274 ± 0.032 Ma. They were thus deposited during the same time period, a finding consistent with the presence of a very similar paleofauna (Table 1). Heavy mineral contents in the Mont Coupet slope deposits are dominated by kaersutitic amphibole, magnetite and titanite, a mineralogy identical to that observed in the Chilhac samples, further supporting a common origin for the Plinian deposit that was reworked at both sites (same eruption or clustered eruptions belonging to the same eruptive phase). Our age is consistent with the 2.14 ± 0.18 Ma age of a basanitic lava flow associated with the Mount Coupet activity (Fouris et al., 1991), providing that the flow was emplaced during the older

2.32-2.24 part of the age bracket since the fossil-bearing slope deposits must be younger than the volcanic activity. Together with Chilhac, Mont-Coupet is one of the last occurrence of *Anancus arvernensis* (a forest-dwelling species), replaced by *Mammuthus meridionalis* (an open land species) in younger sites. Global cooling and the advent of glacial cycles starting at about 2.5 Ma in Western Europe (e.g., Shackleton et al., 1984, Kahlke et al., 2011) resulted in the progressive disappearance of large forests, replaced by a more open landscape. The two biotopes still coexisted in the Chilhac and Coupet area around 2.27 Ma.

4.2.3. Senèze fossil deposits

The upper slope deposit sampled in this study is dated at 2.100 ± 0.029 Ma, consistent with an age younger than 2.104 ± 0.050 Ma for some of the recent fossil finds (Nomade et al., 2014b). A second fossil layer dated between 2.176 ± 0.032 Ma and 2.132 ± 0.042 Ma by Nomade et al. (2014b), also provides consistent ages within errors. Whether these fossil layers were deposited at the same time, or indicate a longer duration for the deposition process, or two different faunae are present as suggested by Azaoli et al. (1997), is beyond the scope of this study.

4.2.4. Blassac-La Girondie sand

The site of Blassac-La Girondie is the richest French fossil site of the MNQ19 period, and its age can put key constraints on the beginning of this biozone. Sediments collected inside the fossil deposit give an age of 1.946 ± 0.029 Ma, in agreement with previous rough estimates based on the local geology (Bœuf et al. 1992). This new data, however, favors an old age for the beginning of the MNQ19, which would start much earlier than the younger 1.47 Ma age proposed for the Peyrolles MNQ 19 reference fossil deposit (Nomade et al. 2014b). The sedimentary zircons could possibly be tied to pyroclastic deposits from the central part of the Guéry stratovolcano (La Morangie tephra, dated

at 1.92 ± 0.04 Ma by Féraud et al., 1990), however, a detailed correlation between distal sedimentary deposits and proximal units is beyond the scope of this study.

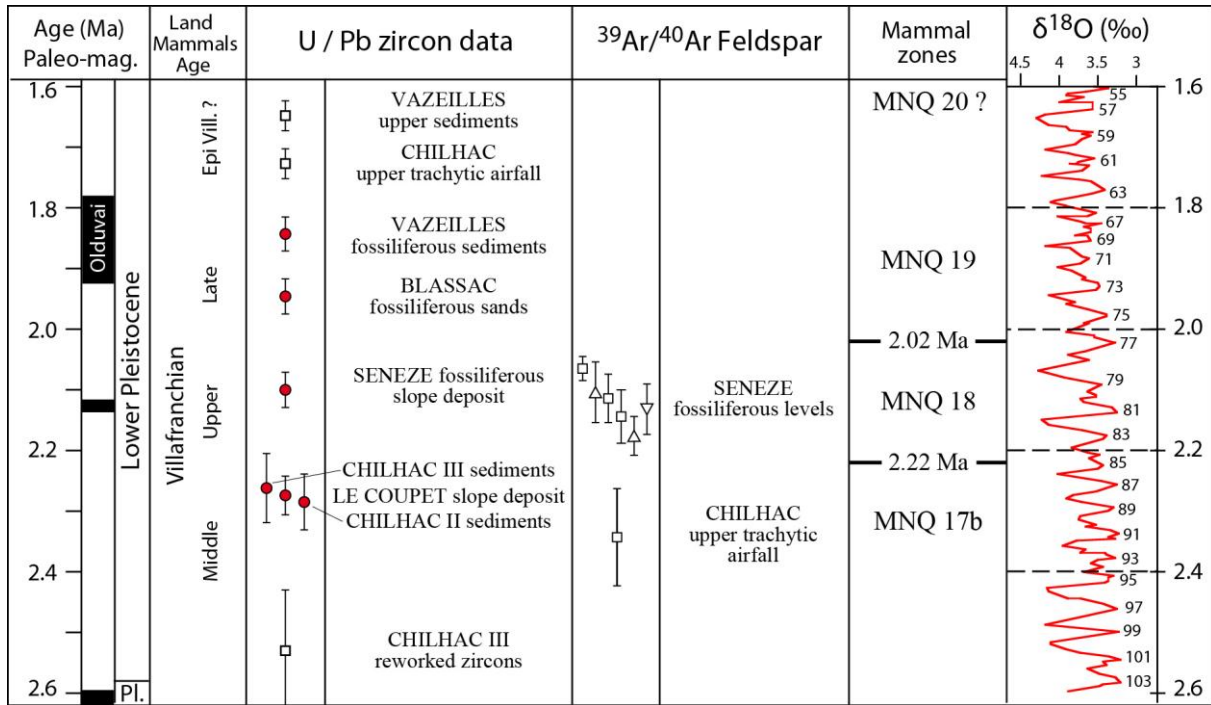


Figure 6: comparison of our new ages with existing ages for the Senèze and Chilhac deposits, European land mammal zones, paleomagnetic chrons, and oxygen isotope variations. U/Pb ages from this study, Ar/Ar ages from Nomade et al. (2014b) and Roger et al. (2000). Red circles are ages of fossiliferous sediments, white triangles ages of tephra-bearing layers above (down-pointing) or below (up-pointing) fossiliferous sediments, and squares for non-fossiliferous sediments or tephra-bearing layers disconnected from the fossil deposits.

4.2.5. Vazeilles sediments

The Vazeilles fossiliferous sediments, dated at 1.818 ± 0.028 Ma, are slightly younger than the Blassac-La Girondie deposit. This age is consistent with the normal polarity of the sediments (Olduvai subchron between 1.925 and 1.780 Ma, Thouveny 1983). Only preliminary paleontological investigations have been performed on this site (Séguy 1974), however, the new age places this site

497 firmly within the MNQ19 biozone. Given the paucity of fossil sites belonging to this time period in
498 central France, this poorly known site is thus of significant interest for the understanding of faunal
499 evolution during the late Villafranchian and would be worth further investigation. The sedimentary
500 sequence could also provide a record of at least 200 ka of geologic history since the top of the
501 sequence has been dated around 1.648 ± 0.025 Ma.

503 *4.3. Age constraints on late Villafranchian mammal biozones*

504 4.3.1. Duration of the MNQ18 biozone

505 The new U-Pb zircon dating places further constraints on the age and duration of faunal biozones
506 in Central France. The five investigated neighboring sites provide a ~500 ka record of land mammal
507 evolution during the Middle Villafranchian (2.3-1.8 Ma), including significant faunal changes.

508 - The transition between biozones MNQ17b (latest site Chilhac III at 2.262 ± 0.057 Ma) and
509 MNQ18 (earliest possible age for the Senèze fossil deposits at 2.176 ± 0.032 Ma, Nomade et al.
510 2014b) is precisely constrained at 2.22 ± 0.09 Ma.

511 - The transition between biozones MNQ18 (latest fossiliferous level from Senèze at 2.100 ± 0.029
512 Ma) and MNQ19 (Blassac-La Girondie at 1.946 ± 0.029 Ma) is precisely constrained at 2.02 ± 0.10
513 Ma.

514 These two boundaries are consistent with paleomagnetic constraints from the MNQ18 faunae
515 Fonelas P-1 and Puebla de Valverde from Spain (Sinusà et al. 2004, Arribas et al. 2009), which were
516 deposited during the inverse polarity period separating the Réunion and Olduvai normal subchrons, i.e.
517 between 2.116 and 1.925 Ma. They would also be consistent with a possible equivalence between
518 MNQ18 and the Olivola F.U. of Italy dated around 2.10 ± 0.05 Ma (Napoleone 2013), as suggested by
519 Rook et al. (2010).

520 The average duration of the MNQ18 biozone is 200 ka, with a maximum possible duration of
521 400ka, the maximum permissible time between the MNQ17b Chilhac III deposit (2.262 ± 0.057 Ma)
522 and the MNQ19 Blassac-La Girondie deposit (1.946 ± 0.029 Ma).

524 4.3.2. Age of the MNQ19 biozone

525 Only a small number of fossil sites have been attributed to the MNQ19 biozone in Central France.
526 Aside from the reference locality of Peyrolles (Heintz et al. 1974, Valli et al. 2006), the only sites are
527 Blassac-La Girondie and La Sartanette (Palombo and Valli 2004). The age of the Peyrolles deposit has
528 been estimated at 1.40 ± 0.20 Ma (Lo Bello 1988), and further refined at 1.449 ± 0.024 Ma (Nomade et
529 al. 2014b) based on indirect evidence from neighboring pyroclastic deposits. Paleomagnetism data
530 constrain the age of the sediments at La Sartanette to the Olduvai-Jaramillo inverse polarity interval
531 (Thouveny et al. 1984), i.e. between 1.78 and 1.07 Ma. A statistical study by Palombo et al. (2006)
532 confirms the similarity of the Peyrolles and Blassac-La Girondie fauna - La Sartanette was not
533 included in their analysis.

534 The 1.946 ± 0.028 Ma age of the Blassac-La Girondie site thus indicates that the MNQ19 biozone
535 started much earlier than previously thought and solves the mystery of the absence of paleontological
536 deposits in Central France between 2.1 and 1.5 Ma. However, existing ages for Blassac-la Girondie
537 and Peyrolles, would suggest a very long duration for the MNQ19 biozone of about 500 ka. This
538 period corresponds to at least two, possibly three Italian faunal units (Tasso F.U. dated around 1.7-1.8
539 Ma; Farneta F.U. dated around 1.6-1.7 Ma, and probably also Pirro F.U., Napoleone et al. 2013). This
540 time period is still poorly known in Central France, and further research is needed to understand
541 mammal evolution during the late Villafranchian.

542 543 *4.4. Implications for the tephrostratigraphy of the Mont-Dore stratovolcano*

544 The precise chronology of the Mont-Dore stratovolcano during the early Pleistocene is still poorly
545 constrained. Following the major destructive stage that produced a series of four debris avalanches or
546 debris flows (Bernard et al. 2009) at ~2.6 Ma (Cantagrel and Briot 1990, Nomade et al. 2014b), Pastre
547 and Cantagrel (2001) identified at least five major pyroclastic phases during their « middle trachytic
548 cycle » (G3 and G4 cycles of Nomade et al. 2014a). The sites investigated in this study provide an
549 excellent record of the distal tephrochronology of the Mont-Dore stratovolcano during that period and
550 show the existence of at least nine distal tephra deposits that were reworked in the fossiliferous
551 sediments (2.53 ± 0.10 Ma; 2.274 ± 0.032 Ma; 2.176 ± 0.032 Ma; 2.144 ± 0.044 Ma; 2.100 ± 0.029
552 Ma; 1.946 ± 0.029 Ma; 1.818 ± 0.028 Ma; 1.727 ± 0.025 Ma; 1.648 ± 0.025 Ma). This list of nine
553 different pyroclastic events capable of producing distal deposits ~70 km from the Guéry stratovolcano
554 is a conservative estimate since deposits with identical ages might represent different deposits with
555 ages separated by a time shorter than the analytical uncertainty of the U/Pb and $^{40}\text{Ar}/^{39}\text{Ar}$ dating
556 techniques. Four of these pyroclastic events were previously unknown (2.27 Ma; 1.82 Ma; 1.73 Ma;
557 1.65 Ma). The three youngest ages fall within the 1.9 to 1.5 Ma gap between the pyroclastic cycles III
558 and IV of Nomade et al. (2014a) and confirms the observations of Pastre and Cantagrel (2001) of a
559 rather continuous trachytic activity between 2.6 and 1.5 Ma.

561 **5. Conclusions**

562 Given the fast turnover of heavy mineral populations in sediments of the Upper Allier River basin,
563 it is possible to precisely date fossil-bearing sedimentary deposits using U/Pb ages on volcanic zircons
564 originating from Plinian activity of the neighboring Mont-Dore / Guéry stratovolcano. We obtained
565 volcanic zircons ages covering the entire Early Pleistocene, from 2.6 to 1.4 Ma, included during a
566 possible activity gap between pyroclastic cycles III and IV of Nomade et al. (2014a). This indicates
567 that there was no long-duration break in volcanic activity during the history of the volcano.

568 Five paleontological deposits have been precisely dated using U/Pb dating on volcanic zircons.
569 The new data reconciles biochronological and absolute ages for the Chilhac II deposit (2.285 ± 0.046
570 Ma) and a new precise age for Blassac-La Girondie (1.946 ± 0.029 Ma) indicates that the MNQ19
571 biozone started earlier than previously thought. These new U-Pb zircon dates place absolute
572 constraints on the age and duration of the MNQ18 mammal biozone in Central France, and possibly by
573 extension in Western Europe. Since the differentiated volcanic activity in the Mont-Dore area lasted at
574 least from 3.85 to 0.25 Ma (Nomade et al. 2014a), further analyses can be used to provide an absolute
575 geochronological framework for MNQ mammal biozones defined in Central France.

577 **Acknowledgments**

578 The authors are grateful to Claire Fonquernie for her help with mineral separation. We warmly
579 thanked the Doctors Luigi Solari, Albrecht von Quadt and an anonymous reviewer for their helpful
580 corrections and comments as well as the editor Dr. Robyn Pickering for his great efficiency.

581 This research was supported by the French Government Laboratory of Excellence initiative n° ANR-
582 10-LABX-0006. This is Laboratory of Excellence ClerVolc contribution number 453.

584 **References**

585 Arribas, A., Garrido, G., Viseras, C., Soria, J.M., Pla, S., Solano, J.G., Garcés, M., Beamud, E.,
586 Carrión, J.S., 2009. A mammalian lost world in Southwest Europe during the late Pliocene. PLoS ONE
587 4(9), e7127.

588 Aymard, A., 1855. Communication sur la faune du Coupet. Annales de la Société d'Agriculture,
589 Sciences, Arts et Commerce du Puy 20,30-36.

590 Azzaroli, A., 1977. The Villafranchian stage in Italy and the Plio-Pleistocene boundary. In:
591 Neogene–Quaternary Boundary Proceedings II Symposium, Bologna 1975, *Giornale di Geologia* (2)
592 XLI, I–II, 61–79, Bologna.

593 Barbet, P., 2006. Approche taphonomique du site Pliocène terminal de Chilhac (Haute-Loire,
594 France) et étude paléontologique des Cervidae. PhD thesis, Muséum National d’Histoire Naturelle,
595 Paris, 547 pp.

596 Baubron, J.-C., Cantagrel, J.-M., 1980. Les deux volcans des Monts-Dore (Massif Central
597 Français). *Comptes-Rendus de l’Académie des Sciences* 290, 1409-1412.

598 Beden, M., Guth, C., 1970a. Nouvelles découvertes de restes de mammifères dans le gisement
599 villafranchien de Chilhac (Haute-Loire). *Comptes Rendus de l’Académie des Sciences, série D*, 270,
600 2065-2067.

601 Beden, M., Guth, C., 1970b. Un nouveau gisement de vertébrés du Villafranchien de la vallée de
602 l’Allier. *Comptes Rendus de l’Académie des Sciences, série D*, 271, 168-171.

603 Bellucci, L., Bona, F., Corrado, P., Magri, D., Mazzini, I., Parenti, F., Scardia, G., Sardella, R.,
604 2014. Evidence of late Gelasian dispersal of African fauna at Coste San Giacomo (Anagni Basin,
605 central Italy): Early Pleistocene environments and the background of early human occupation in
606 Europe. *Quaternary Science Reviews* 96, 72-85.

607 Bernard, B., van Wyk de Vries, B., Leyrit, H., 2009. Distinguishing volcanic debris avalanche
608 deposits from their reworked products: the Perrier sequence (French Massif Central). *Bulletin of*
609 *Volcanology* 71, 1041-1056.

610 Bœuf, O., 1983. Le site Villafranchien de Chilhac (Haute-Loire) France. Etude paléontologique et
611 biochronologique. PhD thesis, Paris VII University, 253 pp.

612 Bœuf, O., 1997. A propos de Chilhac, Senèze, Blassac-la-Girondie (Haute-Loire), gisements du
613 Pliocène terminal, leur intérêt biochronologique. *in* Aguilar JP, Legendre S, Michaux J(Eds.),
614 *European Neogene Mammal Chronology, Actes du Congrès Biochrom’97. Mémoires et Travaux de*
615 *l’Ecole Pratique des Hautes Etudes de Montpellier* 21, 661–668.

616 Bœuf, O., Geraads, D., Guth, C., 1992. Cervidés villafranchiens de Blassac-la-Girondie (Haute-
617 Loire, France). *Annales de Paléontologie* 78(3), 159-187.

618 Boivin, P., Barbet, P., Bœuf, O., Devouard, B., Besson, J.-C., Hénot, J.-M., Devidal, J.-L.,
619 Constantin, C., Charles, L., 2010. Geological setting of the lower Pleistocene fossil deposits of Chillac
620 (Haute-Loire, France). *Quaternary International* 223-224, 107-115.

621 Boule, M., 1892a. Description géologique du Velay. *Bulletin des Services de la Carte géologique*
622 *de la France* 28, 1-259.

623 Boule, M., 1892b. Découverte d'un squelette d'Elephas meridionalis dans les cendres basaltiques
624 du volcan de Senèze (Haute-Loire). *Comptes Rendus Hebdomadaires des Séances de l'Académie des*
625 *Sciences* 115, 624-626.

626 Bout, P., 1960. Le Villafranchien du Velay et du bassin hydrographique supérieur et moyen de
627 l'Allier, corrélations françaises et européennes. PhD Thesis, Imprimerie Jeanne d'Arc, Le Puy-en-
628 Velay, Haute-Loire, 344 pp.

629 Bout, P., 1970. Absolute ages of some volcanic formations in the Auvergne and Velay areas and
630 chronology of the European Pleistocene. *Palaeogeography Palaeoclimatology Palaeoecology* 8, 95-
631 106.

632 Cantagrel, J.-M., Baubron, J.-C., 1983. Chronologie des éruptions dans le massif volcanique des
633 Monts Dore (méthode potassium-argon), Implications volcanologiques. *Géologie de la France* 2, 123-
634 142.

635 Cantagrel, J.-M., Briot, D., 1990. Avalanches et coulées de débris: le volcan du Guéry; où est la
636 caldeira d'effondrement dans le Massif des Monts Dore? *Comptes Rendus de l'Académie des Sciences*
637 *Paris* 311(II), 219-225.

638 Carbonell, E., Bermúdez de Castro, J.M., Parés, J.M., Pérez-González, A., Cuenca-Bescós, G.,
639 Ollé, A., Mosquera, M., Huguet, R., van der Made, J., Rosas, A., Sala, R., Vallverdú, J., García, N.,
640 Granger, D.E., Martín-Torres, M., Rodríguez, X.P., Stock, G.M., Vergès, J.M., Allué, E., Burjachs,

641 F., Cáceres, I., Canals, A., Benito, A., Díez, C., Lozano, M., Mateos, A., Navazo, M., Rodríguez, J.,
642 Rosell, J., Arsuaga, J.L., 2008. The first hominin of Europe. *Nature* 452, 465-469.

643 Chelle-Michou, C., Laurent, O., Moyen, J.-F., Block, S., Paquette, J.-L., Couzinié, S., Gardien, V.,
644 Vanderhaeghe, O., Villaros, A., Zeh, A., 2017. Pre-Cadomian to late-Variscan odyssey of the eastern
645 Massif Central, France: Formation of the West European crust in a nutshell. *Gondwana Research* 46,
646 170-190.

647 Cohen, K.M., Gibbard, P.L., 2019. Global chronostratigraphical correlation table for the last 2.7
648 million years, version 2019 QI-500. *Quaternary International* 500, 20-31.

649 Couthures, J., Pastre, J.-F., 1983. Chronostratigraphie du Plio-pléistocène d’Auvergne et du
650 Velay: nouveaux apports des datations radiométriques et du paléomagnétisme. *Bulletin de*
651 *l’Association Française pour l’Etude du Quaternaire* 1, 9-18.

652 Couzinié, S., Laurent, O., Chelle-Michou, C., Bouilhol, P., Paquette, J.-L., Gannoun, A.-M.,
653 Moyen, J.-F., 2019. Detrital zircon U–Pb–Hf systematics of Ediacaran metasediments from the French
654 Massif Central: consequences for the crustal evolution of the north Gondwana margin. *Precambrian*
655 *Research* 324, 269-284.

656 Debard, E., Pastre, J.-F., 2004. Le Maar de Senèze, géologie. *in* Pastre, J.-F. (Ed.), *Quaternaire et*
657 *Volcanisme en Auvergne et Velay*, livret-guide de l’excursion AFEQ, mai 2004, pp. 102-108.

658 Delson, E., Faure, M., Guérin, C., Aprile, L., Blackwell, B.A.B., Debard, E., Harcourt-Smith, W.,
659 Martine-Suarez, E., Monguillon, A., Parenti, F., Pastre, J.-F., Sen, S., Skinner, A.R., Swisher III, C.C.,
660 Valli, A.M.F., 2006. Franco-American renewed research at the Late Villafranchian locality of Senèze
661 (Haute-Loire, France). *Cour. Forschungs-Institute Senckenberg* 256, 275-290.

662 Depéret, C., Mayet, L., Roman, F., 1923. Les éléphants pliocènes. 1ère partie: *Elephas planifrons*
663 *Falconer* des sables de Chagny et faunes de mammifères d’âge villafranchien Saint-Prestien. 2ème
664 partie: monographie des éléphants pliocènes d’Europe et d’Afrique du Nord. *Annales de l’Université*
665 *de Lyon I, Sciences-Médecine*, fasc. 42.

666 de Vos, J., Mol, D., Reumer, W.F., 1995. Early Pleistocene cervidae (Mammalia, Artiodactyla)
667 from the Oosterschelde (the Netherlands), with a revision of the cervid genus *Eucladoceros* Falconer,
668 1868. *Deinsea*, 2, 21-95.

669 Dorlhac, M.J., 1854. Notice sur le cratère de Coupet et sur son gisement de gemmes et
670 d'ossements fossiles. *Annales de la Société d'Agriculture, Sciences, Arts et Commerce du Puy* 19, 497-
671 517.

672 Elhaï, H., 1969. La flore sporo-pollinique du gisement villafranchien de Senèze (Massif central,
673 France). *Pollen et Spores* 11(1), 127-139.

674 Féraud, G., Lo Bello, P., Hall, C.M., Cantagrel, J.-M., York, D., Bernat, M., 1990. Direct dating of
675 Plio-Quaternary pumices by $^{40}\text{Ar}/^{39}\text{Ar}$ step-heating and single-grain laser fusion methods: the example
676 of the Monts-Dore massif (Massif Central, France) *Journal of Volcanology and Geothermal Research*
677 40, 39-53.

678 Fouris, M., Cantagrel, J.M., Poidevin, J.L., Mergoil, J., 1991. Le Plio-pléistocène du Velay:
679 volcanologie et chronologie K/Ar des gisements fossilifères. Données actuelles, problèmes et
680 hypothèses. *in* Datation et caractérisation des milieux Pléistocènes. Actes des symposiums 11 et 17 de
681 la 11ème Réunion Annuelle des Sciences de la Terre, Clermont-Ferrand, 1986. *Cahiers du Quaternaire*
682 16, 401-416.

683 Garcés, M., Agustí, J., Parés, J.M., 1997. Late Pliocene continental magnetochronology from the
684 Guadix-Baza Basin (Betic Ranges, Spain). *Earth Planet. Sci. Lett.* 146(3-4), 677-688.

685 Girod, M., Bouiller, R., Weber, F., Larqué, P., Giot, D., 1979. Geological map of France
686 (1/50,000), Le Puy en Velay sheet (791).Orléans: BRGM

687 Guérin, C., 1982. Première biozonation du Pléistocène européen, principal résultat
688 biostratigraphique de l'étude des Rhinocerotidae (Mammalia, Perissodactyla) du Miocène terminal au
689 Pléistocène supérieur d'Europe occidentale. *Geobios* 15(4), 593-598.

690 Guérin, C., 1990. Biozones or mammal units? Methods and limits in biochronology. In: Lindsay
691 EH, Fahlbusch V, Mein P (Eds.), *European Neogene Mammal Chronology*. Plenum Press Edit., New

692 York, (NATO Advanced Research Workshop “European Neogene Mammal Chronology” Munich,
693 Mai 1988), 119-130.

694 Guérin, C., 2007. Biozonation continentale du Plio-pléistocène d’Europe et d’Asie occidentale par
695 les mammifères: état de la question et incidence sur les limites Tertiaire/Quaternaire et
696 Plio/Pléistocène. *Quaternaire* 18(1), 23-33.

697 Guérin, C., Faure, M., Argant, A., Argant, J., Crégut-Bonnoure, E., Debard, E., Delson, E.,
698 Eisenmann, V., Hugueney, M., Limondin-Lozouet, N., Martin-Sufirez, E., Mein, P., Mourer-Chauviré,
699 C., Parenti, F., Pastre, J.-F., Sen, S., Valli, A.M.F., 2004. Le gisement pliocène supérieur de Saint-
700 Vallier (Drôme, France) : synthèse biostratigraphique et paléoécologique. *Geobios* 37, S349-S360.

701 Guth, C., 1974. Découverte dans le Villafranchien d’Auvergne de galets aménagés. *Comptes*
702 *Rendus de l’Académie des Sciences Paris* 279, 1071-1072.

703 Guth, C., 1975. Chilhac et Blassac-La Girondie, deux gisements Villafranchiens de la vallée de
704 l’Allier. Colloque CNRS 218, 4-9 juin 1973: Problèmes actuels de paléontologie – Evolution des
705 vertébrés, 627-630.

706 Guth, C., Chavaillon, J., 1985. Découverte en 1984 de nouveaux outils paléolithiques à Chilhac III
707 (Haute-Loire). *Bulletin de la Société Préhistorique Française* 82, 56-64.

708 Heintz, E., Guérin, C., Martin, P., Prat, F., 1974. Principaux gisements Villafranchiens de France :
709 listes fauniques et biostratigraphie. *Mémoires du BRGM* 78, 411-417.

710 Hiess, J., Condon, D.J., McLean, N., Noble, S.R., 2012. $^{238}\text{U}/^{235}\text{U}$ systematics in terrestrial
711 uranium-bearing minerals. *Science* 335, 1610-1614.

712 Horstwood, M.S.A., Košler, J., Gehrels, G., Jackson, S., McLean, N., Paton, C., Pearson, N.J.,
713 Sircombe, K., Sylvester, P., Vermeesch, P., Bowring, J.F., Condon, D.J., Schoene, B., 2016.
714 Community-derived standards for LA-ICP-MS U-(Th-)Pb geochronology – Uncertainty propagation,
715 Age interpretation and data reporting. *Geostandard and Geoanalytical Research*, 40, 3, 311-332.

716 Hurai, V., Paquette, J.-L., Huraiová, M., Konečný, P., 2010. U–Th–Pb geochronology of zircon
717 and monazite from syenite and pincinite xenoliths in Pliocene alkali basalts of the intra-Carpathian
718 back-arc basin. *Journal of Volcanology and Geothermal Research* 198, 275-287.

719 Jackson, S.E., Pearson, N.J., Griffin, W.L., Belousova, E.A., 2004. The application of laser
720 ablation-inductively coupled plasma-mass spectrometry to in situ U–Pb zircon geochronology.
721 *Chemical Geology* 211, 47–69.

722 Jaffrey, A.H., Flynn, K.F., Glendenin, L.E., Bentley, W.C., Essling, A.M., 1971. Precision
723 measurements of half-lives and specific activities of U^{235} and U^{238} . *Physical Reviews*, C4, 1889.

724 Kahlke, R.D., García, N., Kostopoulos, D.S., Lacombe, F., Lister, A.M., Mazza, P.P.A., Spassov,
725 N., Titov, V.V., 2011. Western Palaeartic palaeoenvironmental conditions during the Early and early
726 Middle Pleistocene inferred from large mammal communities, and implications for hominin dispersal
727 in Europe. *Quaternary Science Reviews* 30, 1368-1395.

728 Lasnier B., Marchand, J., Bouiller, R., Cornen, G., Burg, J.-P., Forestier, F.-H., Leyreloup, A.,
729 1981. Geological map of France (1/50,000), Brioude sheet (766).Orléans: BRGM.

730 Ledru, P., Vitel, G., Beurrier, M., Marchand, J., Dallain, C., Turland, M., Etlicher, B., Dautria, J.-
731 M., Liotard, J.-M., 1994. Geological map of France (1/50,000), Craponne-sur-Arzon sheet (767).
732 Orléans: BRGM.

733 Lo Bello, P., 1988. Géochronologie par la méthode ^{39}Ar - ^{40}Ar de ponces quaternaires contaminées:
734 exemple des ponces du Mont-Dore (Massif Central, France). Utilisation d'un laser continu pour la
735 datation des minéraux individuels. PhD thesis, Université de Nice, 122 pp.

736 Lordkipanidze, D., Ponce de León, M.S., Margvelashvili, A., Rak, Y., Rightmire, G.P., Vekua, A.,
737 Zollikofer, C.P.E., 2013. A complete skull from Dmanisi, Georgia, and the evolutionary biology of
738 Early Homo. *Science* 342(6156), 326-331.

739 Ludwig, K.R., 2001. User's manual for Isoplot/Ex Version 2.49, a Geochronological Toolkit for
740 Microsoft EXCEL. Berkeley Geochronological Center, Special Publication 1a, Berkeley, USA (55 pp).

741 Marchand, J., Bouiller, R., Cornen, G., Burg, J.-P., Lasnier B., 1986. Geological map of France
742 (1/50,000), Langeac sheet (790). Orléans: BRGM.

743 Mein, P., 1976, Biozonation du Néogène méditerranéen à partir de mammifères. Proceedings VIth
744 congress R.C.M.N.S., Bratislava 1975.

745 Mercer, C.M., Hodges, K.V., 2016. ArAR - A software tool to promote the robust comparison of
746 K–Ar and $^{40}\text{Ar}/^{39}\text{Ar}$ dates published using different decay, isotopic, and monitor-age parameters.
747 Chemical Geology 440, 148-163.

748 Mergoïl, J., Boivin, P., 1993. Le Velay. Son volcanisme et les formations associées. Géologie de
749 la France 3, 1–96.

750 Mossand, P., Cantagrel, J.-M., Vincent, P., 1982. La caldera de Haute Dordogne: âge et limites
751 (Massif des Monts-Dore, France). Bulletin de la Société Géologique de France 24(4),727-738.

752 Napoleone, G., Albanelli, A., Azzaroli, A., Bertini, A., Magi, M., Mazzini, M., 2003. Calibration
753 of the upper Valdarno basin to the Plio-Pleistocene for correlating the Apennine continental sequences.
754 Il Quaternario 16, 131–166.

755 Nehlig, P., Boivin, P., De Goër de Hervé, A., Mergoïl, J., Prouteau, G., Thiéblemont, D., 2001.
756 Les volcans du Massif central. Géologues 66–91.

757 Niespolo, E.M., Rutte, D., Deino, A.N., Renne, P.R., 2017. Intercalibration and age of the Alder
758 Creek sanidine $^{40}\text{Ar}/^{39}\text{Ar}$ standard. Quaternary Geochronology 39, 205-213.

759 Nomade, S., Pastre, J.-F., Nehlig, P., Guillou, H., Scao, V., Scaillet, S., 2014a. Tephrochronology
760 of the Mont-Dore volcanic Massif (Massif Central, France): new $^{40}\text{Ar}/^{39}\text{Ar}$ constraints on the late
761 Pliocene and Early Pleistocene activity. Bull. Volcanol. 76(3), 1–17.

762 Nomade, S., Pastre, J.-F., Guillou, H., Faure, M., Guérin, C., Delson, E., Debard, E., Voinchet, P.,
763 Messager, E., 2014b. $^{40}\text{Ar}/^{39}\text{Ar}$ constraints on some French landmark Late Pliocene to Early
764 Pleistocene large mammalian paleofaunas: Paleoenvironmental and paleoecological implications.
765 Quaternary Geochronology 21, 2-15.

766 Nomade, S., Pastre, J.-F., Pereira, A., Courtin-Nomade, A., Scao, V., 2017. New $^{40}\text{Ar}/^{39}\text{Ar}$
767 constraints for the “Grande Nappe”: The largest rhyolitic eruption from the Mont-Dore Massif
768 (French Massif Central). *Comptes Rendus Geosciences* 349, 71-80.

769 Nomade, S., Scaillet, S., Pastre, J.-F., Nehlig, P., 2012. Pyroclastic chronology of the Sancy
770 stratovolcano (Mont-Dore, French Massif Central): new high-precision $^{40}\text{Ar}/^{39}\text{Ar}$ constraints. *Journal*
771 *of Volcanology and Geothermal Research* 225-226, 1-12.

772 Nomade, S., Scao, V., Guillou, H., Messenger, E., Mgeladze, A., Voinchet, P., Renne, P.R.,
773 Courtin-Nomade, A., Bardintzeff, J.-M., Ferring, R., Lordkipanidze, D., 2016. New $^{40}\text{Ar}/^{39}\text{Ar}$,
774 unspiked K/Ar and geochemical constraints on the Pleistocene magmatism of the Samtskhe-Javakheti
775 highlands (Republic of Georgia). *Quaternary International* 395, 45-59.

776 Palombo, M.R., 2014. Deconstructing mammal dispersals and faunal dynamics in SW Europe
777 during the Quaternary. *Quaternary Science Reviews* 96, 50-71.

778 Palombo, M.R., Sardella, R., 2007. Biochronology and biochron boundaries: a real dilemma or
779 false problem? An example based on Pleistocene large mammalian faunas from Italy. *Quaternary*
780 *International* 160, 30-42.

781 Palombo, M.R., Valli, A.M.F., 2004. Biochronology of large mammal faunas from Pliocene to
782 Middle Pleistocene in France. *Geologica Romana* 37, 145-163.

783 Palombo, M.R., Valli, A.M.F., Kostopoulos, D.S., Alberdi, M.T., Spassov, N., Vislobokova, I.,
784 2006. Similarity relationships between the Pliocene to Middle Pleistocene large mammal faunas of
785 Southern Europe from Spain to the Balkans and the North Pontic Region. *Cour. Forsch.-Inst.*
786 *Senckenberg* 256, 329-347.

787 Paquette, J.-L., Médard, E., Francomme, J.E., Bachèlery, P., Hénot, J.-M., 2019. LA-ICP-MS
788 U/Pb zircon timescale constraints of the Pleistocene latest magmatic activity in the Sancy
789 stratovolcano (French Massif Central). *Journal of Volcanology and Geothermal Research* 374, 52-61.

790 Paquette, J.-L., Piro, J.-L., Devidal, J.-L., Bosse, V., Didier, A., Sannac, S., Abdelnour, Y., 2014.
791 Sensitivity enhancement in LA-ICP-MS by N₂ addition to carrier gas: application to radiometric dating
792 of U-Th-bearing minerals. *Agilent ICP-MS Journal* 58, 4-5.

793 Pareto, L., 1865. Note sur les subdivisions que l'on pourrait établir dans les terrains tertiaires de
794 l'Apennin septentrional. *Bulletin de la Société Géologique de France* 22, 210–277.

795 Pastre, J.-F., 1987. Les formations plio-quaternaires du Bassin de l'Allier et le volcanisme
796 régional (Massif Central, France). PhD thesis, Université Pierre et Marie Curie, Paris, 706 pp.

797 Pastre, J.-F., Cantagrel, J.-M., 2001. Téphrostratigraphie du Mont Dore (Massif Central, France).
798 *Quaternaire* 12 (4), 249–267.

799 Pastre, J.-F., Debard, E., Nomade, S., Guillou, H., Faure, M., Guérin, C., Delson, E., 2015.
800 Nouvelles données géologiques et téphrochronologiques sur le gisement paléontologique du maar de
801 Senèze (Pléistocène inférieur, Massif Central, France). *Quaternaire* 26(3), 225-244.

802 Prévot, M., 1975. Magnétisme et minéralogie magnétique de roches Néogènes et Quaternaires,
803 contribution au paléomagnétisme et à la géologie du Velay. PhD thesis, Université Pierre et Marie
804 Curie Paris VI.

805 Renne, P.R., Balco, G., Ludwig, K.R., Mundil, R., Min, K., 2011. Response to the comment by
806 W.H. Schwarz et al. on “Joint determination of 40K decay constants and ⁴⁰Ar*/⁴⁰K for the Fish
807 Canyon sanidine standard, and improved accuracy for ⁴⁰Ar/³⁹Ar geochronology” by PR Renne, et al.
808 (2010). *Geochimica et Cosmochimica Acta* 75, 5097-5100.

809 Raynal, J.-P., Magoga L., Bindon, P., 1995. Téphrofacts and the first human occupation of the
810 French Massif Central. in *The Earliest occupation of Europe*, W. Roebroeks & T. van Kolfschoten Ed.,
811 University of Leiden, 129-146.

812 Roger, S., Coulon, C., Thouveny, N., Féraud, G., Van Velzen, A., Fauquette, S., Cochemé, J.J.,
813 Prévot, M., Verosub, K.L., 2000. ⁴⁰Ar/³⁹Ar dating of a tephra layer in the Pliocene Senèze maar
814 lacustrine sequence (French Massif Central): constraint on the age of the Réunion-Matuyama transition
815 and implication on paleoenvironmental archives. *Earth and Planetary Science Letter* 138, 431-440.

816 Rook, L., Martínez-Navarro, B., 2010. Villafranchian: The long story of a Plio-Pleistocene
817 European large mammal biochronologic unit. *Quaternary International* 219, 134-144.

818 Sakata, S., 2018. A practical method for calculating the U-Pb age of Quaternary zircon:
819 corrections for common Pb and initial disequilibria. *Geochemical Journal* 52, 1-6.

820 Sakata, S., Hirakawa, S., Iwano, H., Danhara, T., Guillong, M., Hirata, T., 2017. A new approach
821 for constraining the magnitude of initial disequilibrium in Quaternary zircons by coupled uranium and
822 thorium decay series dating. *Quaternary Geochronology* 38, 1-12.

823 Schärer, U., 1984. The effect of initial ^{230}Th disequilibrium on young U-Pb ages: the Makalu case.
824 Himalaya. *Earth Planet. Sci. Lett.*, 67, 191-204.

825 Schaub, S., 1943. Die oberpliocäne Säugetierfauna von Senèze (Haute-Loire) und ihre
826 verbreitungs geschichtliche Stellung. *Eclogae Geologicae Helvetiae* 36(2), 270-289.

827 Séguy, R., 1974. Nouvel horizon fossilifère dans le Villafranchien de la Haute-Loire. *Comptes*
828 *Rendus Annuels de l'Association de Paléontologie et de Préhistoire du Musée de Lyon*: 79-80.

829 Shackleton, N.J., Backman, J., Zimmerman, H., Kent, D.V., Hall, M.A., Roberts, D.G., Schnitker,
830 D., Baldauf, J.G., Desprairies, A., Homrighausen, R., Huddleston, P., Keene, J.B., Kaltenback, A.J.,
831 Krumsiek, K.A., Morton, A.C., Murray, J.W., Westberg-Smith, J., 1984. Oxygen isotope calibration of
832 the onset of ice-rafting and history of glaciation in the North Atlantic region. *Nature* 307(5952), 620-
833 623.

834 Sinusà, C., Pueya, E.L., Azanza, B., Pocoví, A., 2004. Datación magnetoestratigráfica del
835 yacimiento paleontológico de la Puebla de Valverde (Teruel). *Geotemas* 6(4), 339-342.

836 Tera, F., Wasserburg, G.J., 1972. U-Th-Pb systematics in three Apollo 14 basalts and the problem
837 of initial Pb in lunar rocks. *Earth and Planetary Science Letters*, 14, 281-304.

838 Thouveny, N., 1983. Etude paléomagnétique de formations du Plio-pléistocène et de l'Holocène
839 du Massif Central et de ses abords. Contribution à la chronologie du quaternaire. PhD thesis,
840 Université Aix-Marseille II, Marseille.

841 Thouveny, N., Taieb, M., Bonnet, A., 1984. Etude magnétostratigraphique du remplissage du
842 Pléistocène inférieur de la grotte de La Sartanette (Remoulins, Gard). Bulletin de la Société
843 Géologique de France 26(6), 1385-1388.

844 Valli, A.M.F., Caron, J.-B., Debard, E., Guérin, C., Pastre, J.-F., Argant, J., 2006. Le gisement
845 paléontologique villafranchien terminal de Peyrolles (Issoire, Puy-de-Dôme, France): résultats de
846 nouvelles prospections. *Geodiversitas* 28(2), 297-317.

847 van Achterbergh, E., Ryan, C.G., Jackson, S.E., Griffin, W.L., 2001. Data reduction software for
848 LA-ICP-MS: appendix. in P.J. Sylvester (Ed.), *Laser Ablation-ICP-mass spectrometry in the Earth
849 Sciences: principles and applications*, MAC Short Courses Series, Ottawa, Ontario, Canada: 239-243.

850 von Quadt, A., Gakkhofer, D., Guillong, M., Peytcheva, I., Waelle, M., Sakata, S., 2014. U-Pb
851 dating of CA/non-CA treated zircons by LA-ICP-MS and CA-TIMS techniques: impact for their
852 geologic interpretation. *Journal of Analytical Atomic Spectrometry*, 29, 1618.

853 Wendt, I., Carl, C., 1985. U/Pb dating of discordant 0.1 Ma old secondary minerals. *Earth Planet.
854 Sci. Lett.*, 73, 278-284.

855 Wiedenbeck, M., Allé, P., Corfu, F., Griffin, W.L., Meier, M., Oberli, F., von Quadt, A., Roddick,
856 J.C., Spiegel, W., 1995. Three natural zircon standards for U-Th-Pb, Lu-Hf, trace element and REE
857 analyses. *Geostandards Newsletter* 19, 1-23.

859 **Figure Captions:**

860
861 Figure 1. Simplified geological map of the investigated area, redrawn from BRGM 1/50 000 maps
862 (Girod et al. 1979; Lasnier et al. 1981; Ledru et al. 1994; Marchand et al. 1986). The Paleozoic
863 basement is partly covered by basanitic lava flows and pyroclasts belonging to the Devès volcanic
864 field. Dashed circles are known maar structures, including the “Fressanges maar” (Vazeilles site,
865 Séguéy 1974) which was not known at the time the geological maps were drawn. Fossiliferous sites are
866 contained within clastic sediments or slope deposits.

867

868 Figure 2. Cross-section of the Vazeilles deposits along the N102 road, redrawn from Séguy (1974).

869

870 Figure 3. U/Pb diagrams for the investigated zircons from Chilhac and Mont Coupet fossils deposits.

871 (a) and (b) are bulk sediments from the Chilhac deposits, (c) is the upper trachytic airfall located 10 m
872 above the Chilhac III deposit, and (d) are slope deposits from Mont Coupet.

873

874 Figure 4. U/Pb diagrams for the investigated zircons from Senèze, Blassac-La Girondie and Vazeilles
875 fossils deposits.

876

877 Figure 5. Older ages measured in pre-Cenozoic zircons from the fossiliferous sediments a) The Tera-
878 Wasserburg plot represents the Proterozoic and Phanerozoic ages; the Concordia diagram in inset
879 shows the Archean ages; b) Cumulative probability ages histogram plot.

880

881 Figure 6: comparison of our new ages with existing ages for the Senèze and Chilhac deposits,
882 European land mammal zones, paleomagnetic chrons, and oxygen isotope variations. U/Pb ages from
883 this study, Ar/Ar ages from Nomade et al. (2014b) and Roger et al. (2000). Red circles are ages of
884 fossiliferous sediments, white triangles ages of tephra-bearing layers above (down-pointing) or below
885 (up-pointing) fossiliferous sediments, and squares for non-fossiliferous sediments or tephra-bearing
886 layers disconnected from the fossil deposits.

887

888 **Tables content:**

889

890 Table 1. Comparative list of large mammals described in the five investigated fossil deposits. The
891 Chilhac list is reproduced from the compilation of Boivin et al. (2010), the Coupet list from Heintz
892 (1974), the Senèze list from the work of Delson et al. (2006), the Blassac list from Beden and Guth
893 (1970b) and Boeuf et al. (1992), and the Vazeilles list from Séguy (1974).

894

895 Table 2. Sample location and U/Pb chronological data for the investigated fossil sites.

896

897 Table 3. Zircon U-Th-Pb data from the dated samples obtained by in situ Laser-Ablation-ICP-MS.

898

899 Supplementary Table S1: LA-ICP-MS U-Th-Pb dating methodology

900

901